JOURNAL OF GEOPHYSICAL RESEARCH, VOL. 96, NO. B3, PAGES 4289–4300, MARCH 10, 1991

Seismic Reflection Studies in Long Valley Caldera, California

ROSS A. BLACK,[1] SHARON J. DEEMER,[2] AND SCOTT B. SMITHSON

Program for Crustal Studies, University of Wyoming, Laramie

Seismic reflection studies in Long Valley caldera, California, indicate that seismic methods may be successfully employed to image certain types of features in young silicic caldera environments. However, near-surface geological conditions within these environments severely test the seismic reflection method. Data quality are degraded by static, reverberation, and band-limiting problems due to these near-surface conditions. In Long Valley, seismic reflection and refraction methods were used to image both the shallow and deep geothermal aquifers within the area. The deep geothermal aquifer, the welded Bishop Tuff, was imaged as a fairly continuous reflector across the western moat of the caldera. Near-surface refraction information indicates that there may be a buried paleochannel system or horst and graben system that could control the shallow geothermal flow pattern. High-amplitude events observed in a wide-angle survey were originally interpreted as reflections from a contemporary magma body. However, a migration of the events utilizing the new generalized cellular migration algorithm indicates that these events are probably reflections from the faults of the caldera ring fracture system. The reflections may be caused by the high acoustic impedance contrast associated with the juxtaposition of relatively low-velocity, low-density, caldera fill against the granite plutons and metasediments of the Sierran basement along this fault system.

INTRODUCTION

Historically, bright events on seismic reflection sections within active extensional areas have been interpreted as magma bodies within the Earth's crust. These interpretations have been made in both continental [*Brocher*, 1981; *Brocher and Phinney*, 1981; *deVoogd et al.*, 1986; *Serpa and deVoogd*, 1987] and oceanic areas [*Herron et al.*, 1978; *Hale et al.*, 1982; *Morton and Sleep*, 1985; *Detrick et al.*, 1987; *Morton et al.*, 1987]. High-amplitude seismic reflection events observed within the upper crust beneath Long Valley have many features in common with events interpreted to be magma reflections by other investigators. However, because of the complicated near-surface geology within the area and the lack of robust methods for calibrating this class of crustal reflectors, such interpretations must be approached with care.

Major silicic caldera complexes represent fundamental structural and thermal anomalies within the lithosphere. These features offer grave volcanic and earthquake hazards during major eruptive phases [*Hermance*, 1985]. Three silicic calderas within the coterminous United States appear to be young enough and large enough to still be potentially active. These calderas are the Yellowstone caldera, the Valles caldera, and the Long Valley caldera [*Bailey et al.*, 1976]. The Long Valley area has the most active recent volcanic eruption history of these three features [*Hermance*, 1985; *Bailey et al.*, 1976] and a number of studies [*Steeples and Iyer*, 1976; *Bailey et al.*, 1976; *Sanders*, 1984; *Hill et al.*, 1985*b*] have suggested the presence of a magma chamber. In order to further quantify this possibility the University of Wyoming seismic crew conducted wide-angle and vertical incidence seismic reflection profiling in the area over a 2 year period from 1984 through 1985. The data from this profiling represents the only high quality seismic reflection data set available within any of the potentially active silicic caldera complexes in the coterminous United States.

This study will utilize this data set to investigate the hypothesis that the recent reactivation of the caldera is due to the presence and recent movement of magma within the upper crust beneath Long Valley caldera. The data will additionally be used to demonstrate both the utility of the seismic reflection technique to investigations within recently active caldera systems and some of the difficulties encountered when trying to image features within the crust in areas of complex near surface geology. In the course of the study, a new technique for three-dimensional (3-D) prestack migration of poorly constrained reflection events was developed. This technique, termed generalized cellular migration (GCM), will also be introduced.

GEOLOGICAL AND GEOPHYSICAL SETTING

The Long Valley caldera is an elliptical depression approximately 32 km by 17 km in extent. The feature lies in the tectonic transition zone between the Basin and Range and Sierra Nevada tectonic provinces in eastern California (Figure 1).

In the early 1980's, evidence for caldera reactivation became overwhelming and a notice of potential volcanic hazards for the Long Valley area was issued by the U.S. Geological Survey (USGS). Evidence included rapid uplift of areas studied by geodetic leveling, and a marked increase in earthquake swarms within the caldera [*Savage et al.*, 1987]. Models for the mechanism causing the reactivation include caldera inflation at shallow crustal levels, possibly due to injection of magmatic material [*Savage et al.*, 1987; *Savage and Cockerham*, 1984]. The geothermal regime within Long Valley is also of primary importance. It has been designated the type locality for hot water

[1]Now at Department of Geology, University of Kansas, Lawrence.

[2]Now at Earthquake Station, University of Bergen, Bergen, Norway.

Paper number 90JB02401.
0148-0227/91/90JB-02401$05.00

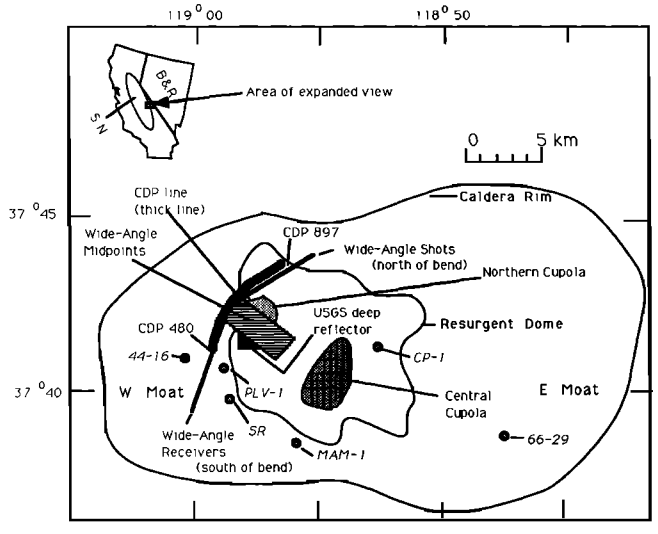

Fig. 1. Location of the Long Valley study area, University of Wyoming seismic experiments, and subsurface features associated with the hypothesized Long Valley magma chamber. The main subsurface features are the upper crustal reflector of *Hill et al.* [1985*a*] (black area), and the *S* wave attenuation zones of *Sanders*, [1984] (stippled areas). The locations of public domain deep well information (heavy dots) are also shown.

geothermal systems by the USGS [*Muffler and Williams*, 1976]. The geometry and extent of the hydrothermal aquifer system are poorly known because of the paucity of drill holes (Figure 1) within the caldera fill. However, the highest temperatures within the geothermal aquifers appear to occur within the deepest caldera fill beneath the western moat [*Sorey*, 1985, 1987]. These high temperatures seem to indicate that a localized body of melt or hot, recently crystallized rock may be present beneath the western moat.

The general geological history of the area has been well summarized by *Bailey et al.* [1976] and *Bailey* [1987]. These studies indicate that the caldera formed approximately 0.7 m.y. ago in a Plinian eruption of a silicic volcano. During this eruption about 650 cubic km of rhyolitic material were ejected along the ring fracture system from a magma chamber at depth. Volcanism occurred in pulses both before and after the catastrophic eruption that formed the caldera. The two most recent events are less than 1000 years in age. About 600 years ago, rhyolitic material was erupted from several small centers along the linear trend of the Mono-Inyo Craters chain. This group of eruptive centers extends from the western moat of the caldera northward into the Mono Basin [*Bailey et al.*, 1976; *Fink*, 1985]. As recently as 200 years ago there was subaqueous extrusive activity beneath Mono Lake, within the Mono Basin [*Hermance*, 1985]. After the main eruption the caldera was filled with postcaldera volcanics, alluvial and lacustrine sediments, and thin glacial deposits.

The hydrologic and geothermal systems have been described by *Lachenbruch et al.* [1976], *Sorey et al.* [1978], *Blackwell* [1985], *Sorey* [1985, 1987], and *Sumnicht and Varga* [1987]. The geothermal system is basically a three-level system. In the western moat waters with temperatures in excess of 200°C occur at depths of nearly a kilometer within the welded Bishop Tuff aquifer. Near the western edge of the resurgent dome a portion of the geothermal water is forced up along faults into a shallow aquifer at a depth of about 100 m.

The general subsurface velocity structure beneath the area has been described by *Steeples and Iyer* [1976], *Hill* [1976], and *Hill et al.* [1985*a*], utilizing teleseismic *P* wave delays and extensive seismic refraction data, respectively. Shear wave attenuation zones were identified in the upper 10 km of the crust by *Sanders* [1984] using *S* wave phases from local earthquakes. *Hill et al.* [1985*a*] interpreted a deep "magma" reflector at a depth of about 7 km near the northernmost of these shear wave attenuation zones (Figure 1). Higher resolution seismic reflection studies have concentrated their efforts in the areas of the caldera identified as anomalous by *Sanders* [1984] and *Hill et al.* [1985*a*]. *Deemer* [1985] and *Berg* [1988] utilized seismic reflection data sets to try to develop a more detailed interpretation of the subsurface in these anomalous areas. This study is an extension of the reflection work by these investigators.

FIELD WORK

Field activities for the seismic reflection experiments discussed here were undertaken during the summer of 1984 by the University of Wyoming seismic reflection crew. The experiments consisted of several noise tests, a standard *P* wave common depth point (CDP) profile, a wide-angle *P* wave expanding spread survey, and limited *P-SV* converted wave tests. These surveys were conducted over the area within the western moat where *Sanders* [1984] identified the northern shear wave attenuation zone (or magma cupola), and where *Hill et al.* [1985*a*] identified a deep intrabasement reflector (Figure 1). The wide-angle experiment was designed specifically to cover the Minaret Summit to Bald Mountain refraction profile conducted by *Hill et al.* [1985*a*].

In all experiments, four *P* wave vibrator trucks (two Mertz model 10 and two Mertz model 11 units) were used to generate the source wavefield. Receiver group arrays consisted of a dozen 10 hz Geosource model MD-81 geophones. Recording spreads consisted of 96 active stations. Data were digitally recorded on a standard 96 channel Geosource MDS-10 recording system.

The noise tests consisted of four small walkaway experiments testing the wave field characteristics in different surficial materials. Walkaway stations were spaced 3 meters apart, with offsets ranging from 21 to 1500 m. Various source and recording configurations were tested. Due to great differences in apparent near-surface attenuation between test sites the noise tests were used to relocate the originally planned CDP line and to slightly modify the originally assumed CDP field parameters [*Deemer*, 1985]. The *P-SV* converted mode tests yielded little information and were not used in the remainder of the study.

A total of about 6 km of nominally 48-fold CDP data were obtained during the 1984 field season (Figure 2). CDP survey station spacings and associated receiver array lengths were both 33 m. The Vibroseis (TM) source consisted of eight 20 s sweeps (10-58 hz) at each station. The vibrators pulled the spread as the survey moved from southwest to northeast. The near-offset gap between source and receivers, as large as 15 stations, was varied during the survey to build up far-offset fold.

Over 13 km of wide-angle coverage was obtained during the field season. An expanding spread geometry was used in the wide-angle survey. Sources and receivers were initially set up at 96 stations 33 m apart, with offsets between 10 km and 13 km. After each set of 10 vibrator sweeps (8-38 hz) both sources and receivers were moved 100 m closer toward the midpoint of the experiment. The source-receiver midpoints were thus concentrated

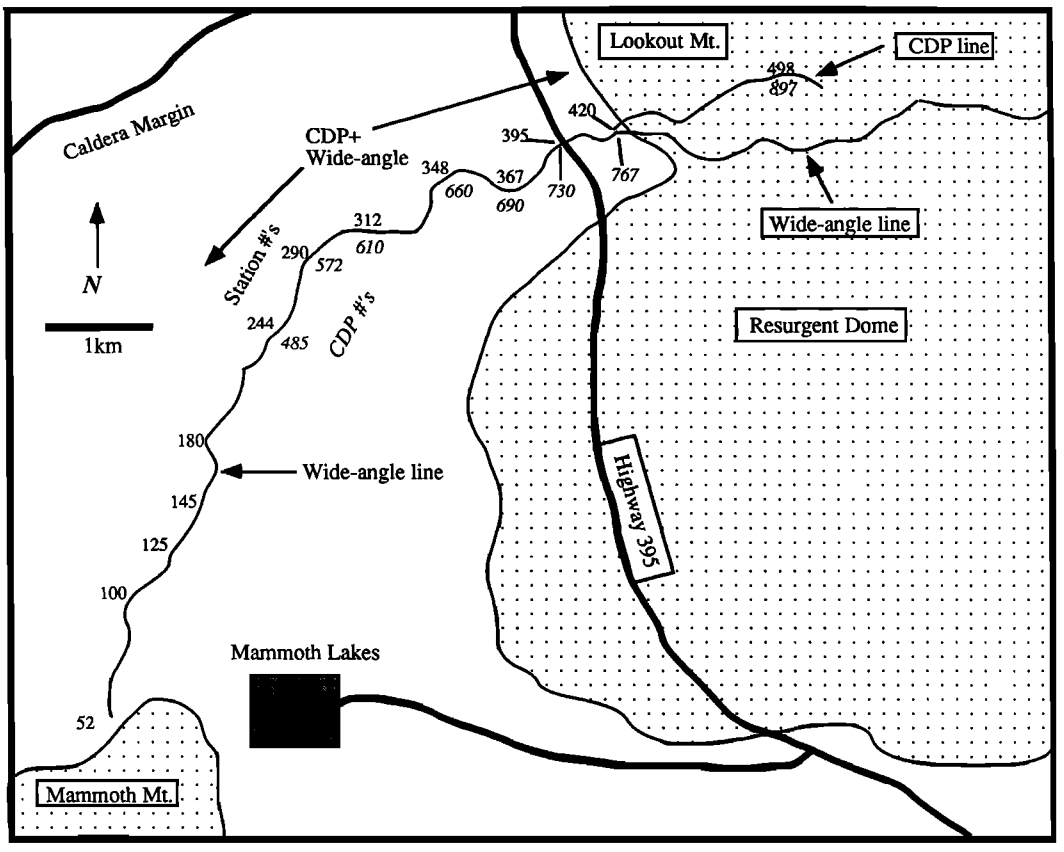

Fig. 2. Detailed location map for the lines used in this study. The CDP locations are shown for the areas with standard CDP coverage. These numbers correspond to the CDP numbers in Figures 3, 5, 7, and 8. The station numbers follow the wide-angle line in the south and the CDP line in the north. In the central portion the stations numbers refer to locations on both lines.

in a relatively small 3 km by 2 km area over *Sanders'* [1984] northern magma cupola (Figure 1). One major advantage of this recording geometry is that the midpoints are spread out in a regularly spaced manner allowing limited 3-D processing of the data.

In general, the data quality was poor in comparison to reflection data gathered with the same type of equipment and field procedures in a sedimentary basin. Although the caldera is topographically a basin, the discontinuous nature of the fill units, the extremely variable near-surface velocity distribution, and the complex structure within the caldera caused extraordinary problems in all phases of the field program. The poor quality of the field data posed great difficulty in the processing and interpretational phases of the project.

PROCESSING AND INTERPRETATION

The seismic reflection data from Long Valley contain several reflection events. Some of these events can be identified on both the wide-angle and CDP data sets and can be correlated with major lithological breaks observed in the sparse deep well data available. Other events have more uncertain origins. Velocity control derived from the stacking velocities is relatively poor due to the discontinuous nature of most of the events. For this reason, extensive use was made of the refraction velocity model developed by *Hill et al.* [1985*a*] for interpretating of the potential reflection events. In addition, useful near-surface information was obtained by analyzing the first-break travel times on individual shot records from the CDP survey.

Hyperbolic events occur on the near-offset records of the wide-angle data at approximately 0.8 to 1.2 seconds of two-way travel time. Similar events occur on the CDP records. These events show up on the stacked section of the CDP line (Figure 3) as a relatively continuous event. The reflector probably represents a fairly continuous geological feature across much of the western moat. The processing sequence leading to the stacked section is given in Figure 4. In Figure 3, the event at about 0.8 s near CDP location 740 is localized and discontinuous. The continuous event degrades near the ends of the line due to loss of fold but also due to the fact that the event amplitude is highest on individual CDP records near the center of the line. An interpreted version of the line (Figure 5) highlights the major events evident on the section. The main reflector is the interface between the Bishop Tuff, the basal caldera fill unit, and the Sierran basement rocks. The 'I' reflector may be a small intrusive unit within the section.

Generalized lithological sections are available from several deep wells in the western to central portion of the caldera (Figures 1 and 6). Although none of these wells are coincident with the seismic lines, they provide the best available structural and stratigraphic control for the seismic data. Approximate two-way, normal incidence travel times to the top of the basement are plotted in Figure 6 next to the lithologic sections. These travel times were calculated using appropriate velocities from the models of *Hill et al.* [1985*a*].

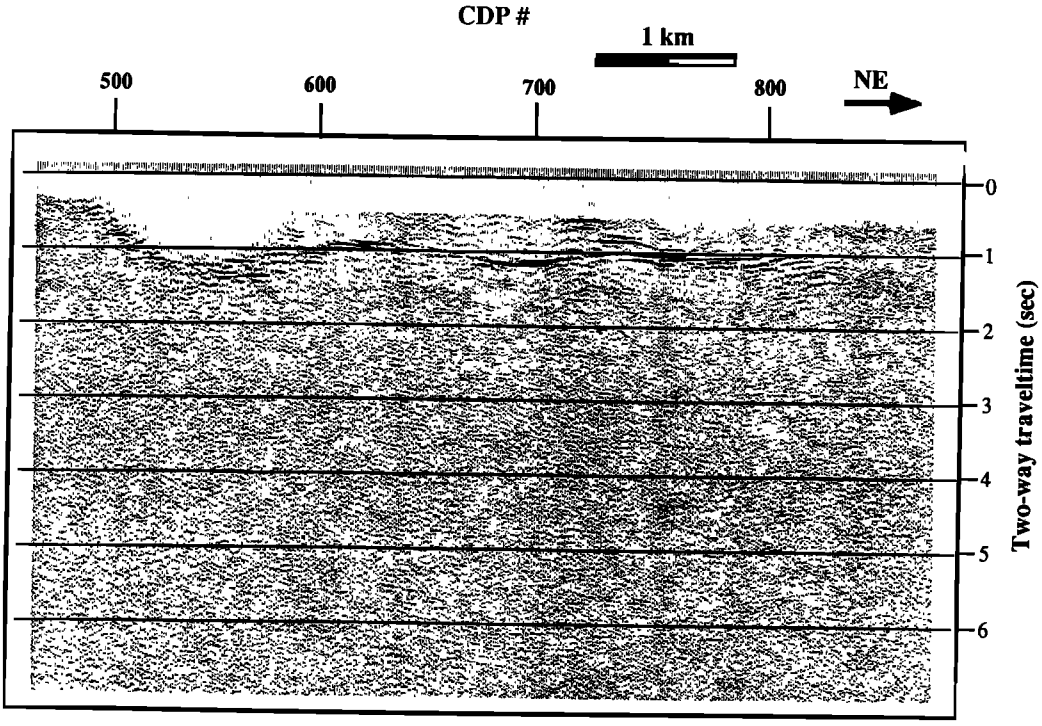

Fig. 3. Stacked section of CDP data. Main reflector is the caldera fill/basement interface. Interpretations of this section are shown in Figures 5 and 7. The horizontal exaggeration is approximately 2:1.

Using the lithologies and depths observed in the well data, an interpreted cross section was made along the CDP line (Figure 7). The continuous reflector observed on the data sets apparently corresponds to the interface between the caldera fill and the precaldera crystalline basement. In this general area of the caldera, then, any true reflection events seen in the seismic data at normal incidence times of greater than 1.2 s must either be true intra-basement reflections, multiple reflections, *P-SV* converted phases reflected from within the caldera fill, or out-of-the-plane, sideswipe reflections.

Final CDP Processing Flow

Tape input
Demultiplex
Cross-correlation
Geometry definition
Refraction analysis
CDP bin relocation
CDP sort
Predictive deconvolution
Frequency filtering
Datum statics correction
Refraction statics correction
Velocity analysis
Residual statics analysis
NMO correction
First break muting
Residual statics correction
CDP stack

Fig. 4. Processing flow used to create stacked CDP seismic section shown in Figure 3.

The interface between the caldera fill and the basement is an extremely important unit in the western moat because it is the main deep geothermal aquifer in the area [*Sorey*, 1987]. The quality of the reflection image (Figure 3) of this interface indicates that seismic reflection surveys could be of great use in identifying structural controls on aquifer characteristics. The discontinuous event at 0.8 s has been interpreted as a possible intrafill intrusive sill because of its shape, small areal extent, a general velocity pull-up below the event, and the fact that similar intrusions are seen in outcrop on upfaulted blocks to the north of the line [*Bailey et al.*, 1976]. In addition, the densities of caldera fill materials examined by *Carle and Goldstein* [1987] indicate that (ignoring intrusive momentum) silicic intrusions would naturally tend to pond at this level in the stratigraphic section due to buoyancy considerations. *Blackwell* [1985] emphasized that the deep geothermal system would have to be thermally recharged occasionally throughout the history of the system in order to maintain the elevated temperatures observed in the aquifer. The interpreted intrusion (Figure 7), and others like it, could have provided a thermal charge directly to the aquifer.

The CDP stacked section provides no information above approximately 500 m in depth (Figure 3) since information from shallower depths must be deleted during processing of the data. However, a refraction statics analysis was performed on the CDP data set using the generalized reciprocal method [*Palmer*, 1981]. This analysis provides some limited information about the near-surface geology. The refraction interpretation along the CDP line (Figure 8) clearly shows the presence of two "bedrock" lows along

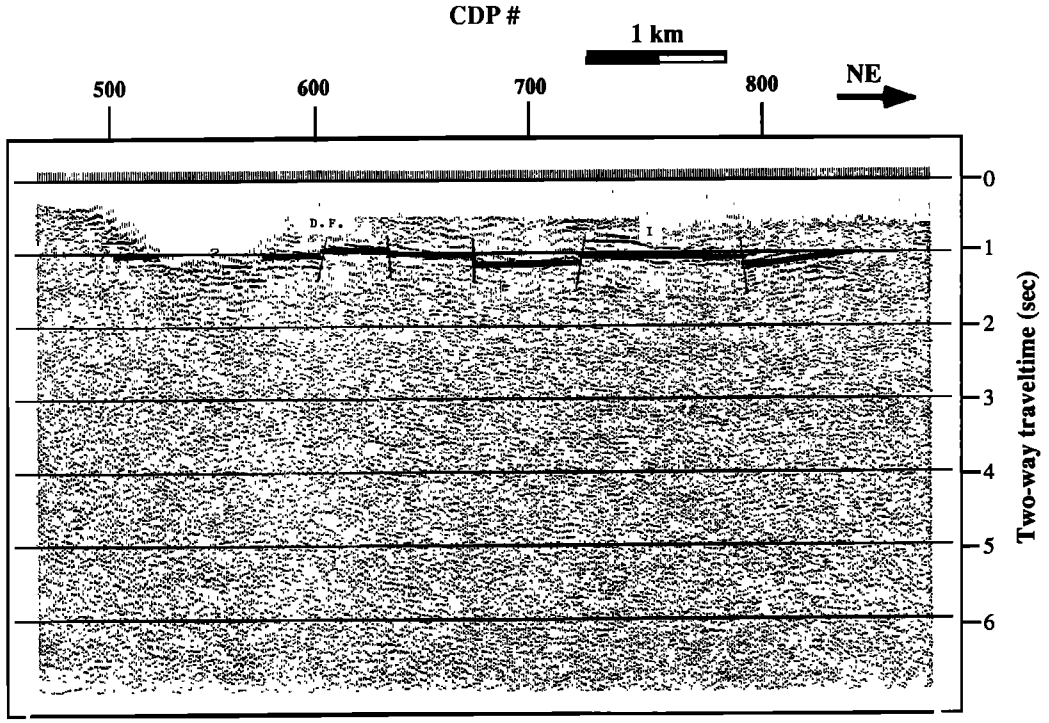

Fig. 5. Interpreted stacked section of CDP data. Main reflector, marked by the near-horizontal solid line, is the caldera fill-basement interface. Event I is the interpreted intrusion. Interpreted faults shown as near-vertical solid lines. D.F. marks approximate area of Discovery Fault, an hypothesized geothermal conduit. The horizontal exaggeration is approximately 2:1.

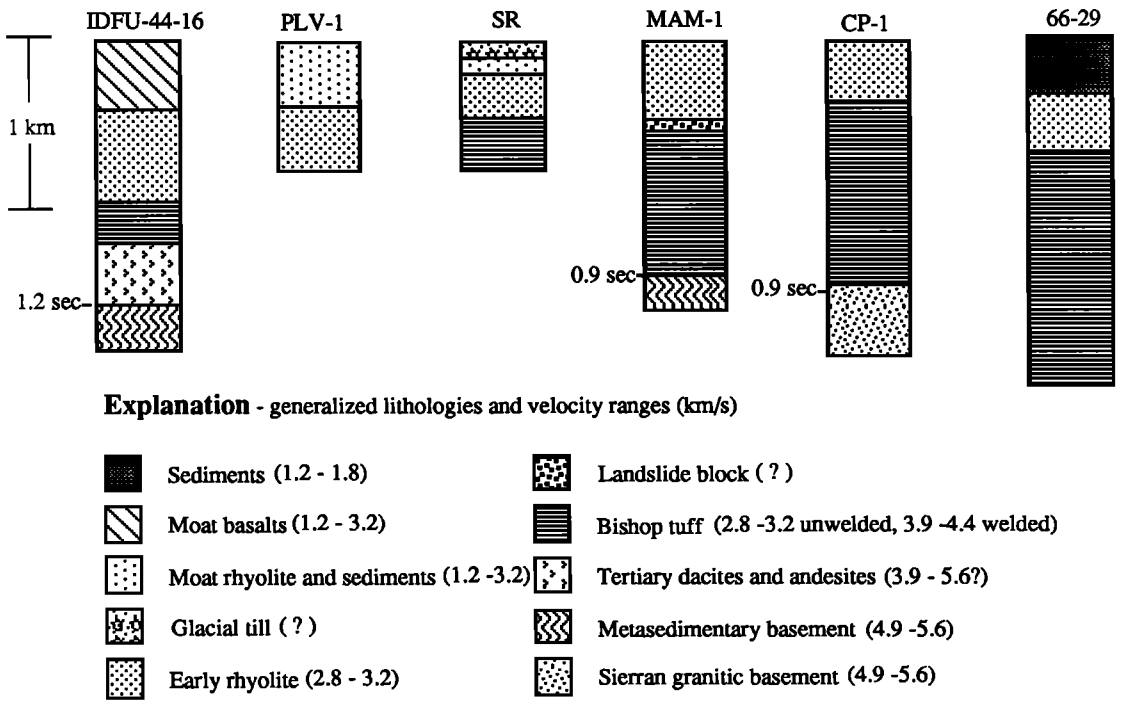

Fig. 6. Generalized lithologic sections from deep wells of Figure 1. Seismic P-wave velocity ranges for generalized lithologies taken from *Hill et al.* [1985*a*], *Deemer* [1985] and *Black* [1990]. Very low velocities generally indicate that the lithology is highly fractured or poorly lithified in the near-surface. Approximate seismic two-way travel times to basement noted on wells penetrating basement lithologies.

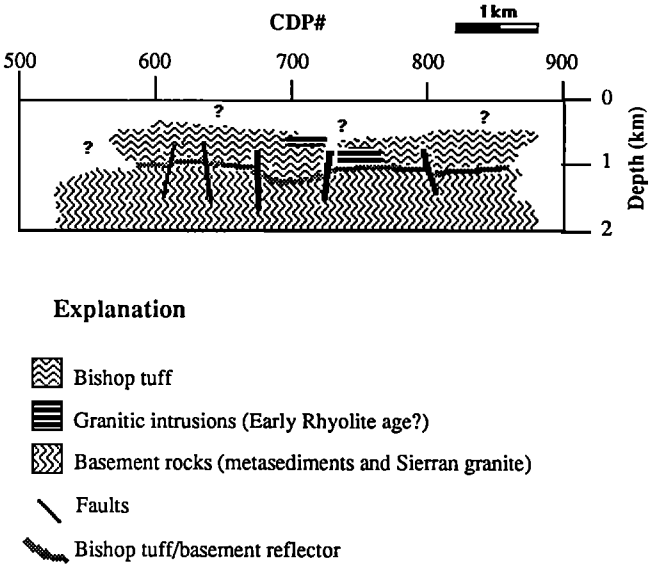

Fig. 7. Schematic geological cross section interpreted from near-vertical-incidence CDP line of Figure 3. Note absence of information above seismic mute zone and within basement. The contact between basement and caldera fill (here it is Bishop tuff) is fairly well defined by the continuous reflector of Figure 3. The intrusions are interpreted from reflection character, velocity considerations, magma dynamic considerations, and nearby outcrop information. There is no drill information to verify this interpretation, however.

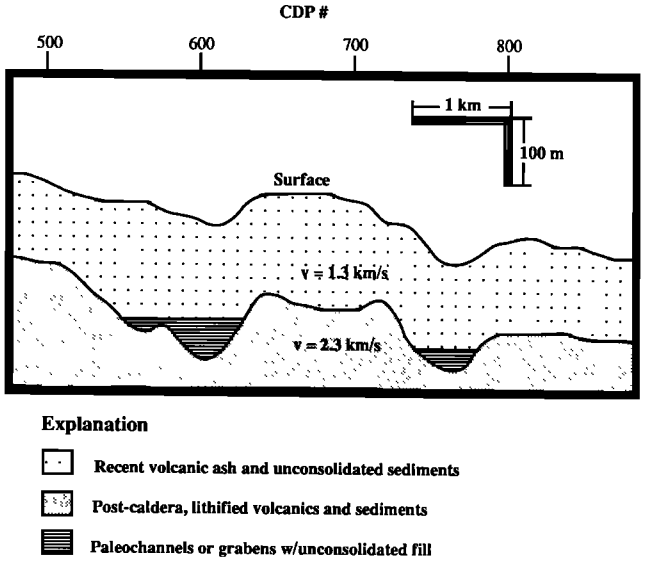

Fig. 8. Near-surface interpretation of first break information from the CDP line. The interpreted paleochannels or graben system could act as conduits for exploitable hydrothermal resources.

the line. These lows can be interpreted as either structural grabens or erosional features such as incised paleochannels. These lows are at the same depth as the shallow hydrothermal aquifer [*Sorey*, 1985, 1987] and may represent preferential flow paths within the aquifer system.

Many high amplitude events are observable on the wide-angle shot records with apparent two-way, normal incidence arrival times of greater than 1.2 seconds (Figure 9). These events were also observed by *Deemer* [1985]. She grouped all such events together as the "slow event" and discussed their possible origin. The possibilities discussed included converted *P-SV* phases, second-arriving refracted phases from volcanics within the caldera fill, ground roll, and sideswipe. Arguments were given to eliminate the possibilities of converted waves and groundroll. Other possible explanations for the identity of the events include that they are true intrabasement reflections or that they are high-amplitude postcritical reflections from within the caldera fill.

Upon examination of common-offset gathers and 3-D CDP gathers, the possibilities of both offset dependent phases (postcritical arrivals) and second arriving refractions can be eliminated because the high-amplitude events are not highly correlated with offset but rather with spatial position (3-D midpoint). On individual shot records (Figure 9) the "slow event" is actually made up of several individual events with different move-outs and wavelet characteristics. These individual events were summarized by *Deemer* [1985]. From her analysis the apparent intercept times for individual events are well below 1.2 s indicating that they could not be individual inline refraction events coming from within the caldera fill.

The remaining possible explanations for the identity of the high amplitude events below 1.2 s are that they are true

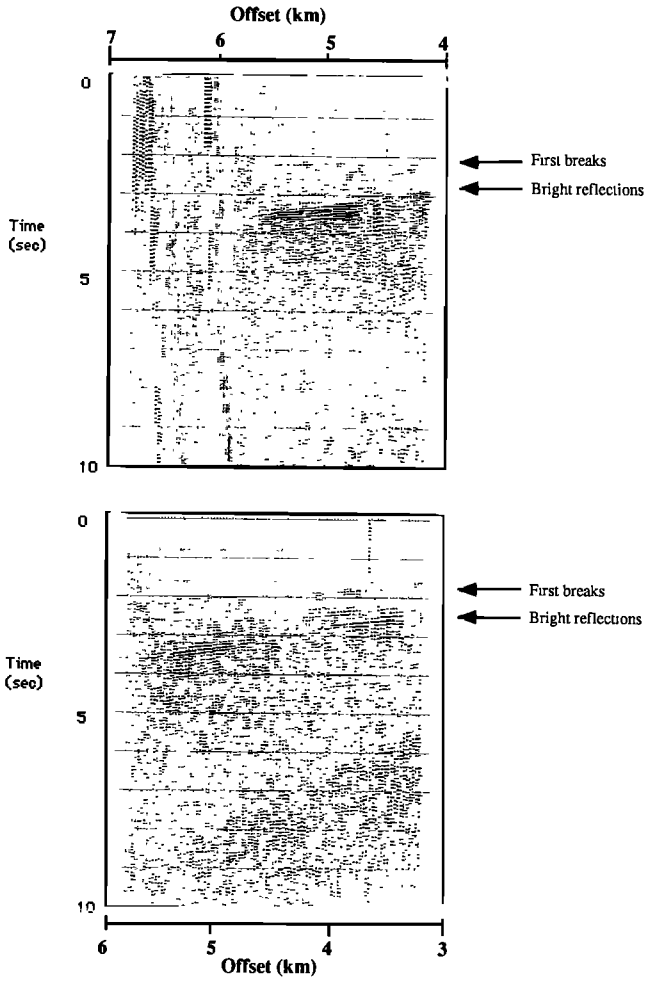

Fig. 9. Wide-angle shot records showing bright reflection events. These events are discontinuous (see time plot on Figure 13) but are the strongest events observed on any of the wide-angle records.

intrabasement reflections or that they are sideswipe reflections from features not centered near the midpoints of the wide-angle line. In either case, the high-amplitude events are probably reflections.

The 1984 wide-angle data were collected with a recording geometry which forced the shot-receiver midpoints to fall within a rectangular area, approximately 2 km by 3 km, in the center of the spread (Figure 1). Because the midpoints were fairly well distributed within this rectangle, sorting of the data traces into evenly distributed midpoint or CDP gathers yielded a data set which could be processed as a 3-D seismic survey. A 30 by 30 bin 3-D CDP grid (Figure 10) was defined within the rectangle. The data were sorted, edited, NMO corrected, corrected for static shifts, muted, and stacked. Stacking velocities (3 to 3.5 km/s) were interpreted from standard velocity panels. Three cross-sectional slices through the 3-D stacked data set (Figure 11), processed to preserve relative amplitude relationships within the seismic section, show that these events are indeed much higher in amplitude than any other energy in the section. However, a generalized time map for the high amplitude events (Figure 10) shows that none of the high amplitude events are spatially continuous across the entire area of CDP coverage. The apparent surface area over which each of the events is observed is much smaller than the first Fresnel zone, indicating, along with the very low stacking velocities, that simple CDP mapping may be an incorrect processing approach. However, because of the very limited 30 trace aperature of the 3-D wide-angle stack, the true spatial position of the bright events cannot be found by conventional migration techniques.

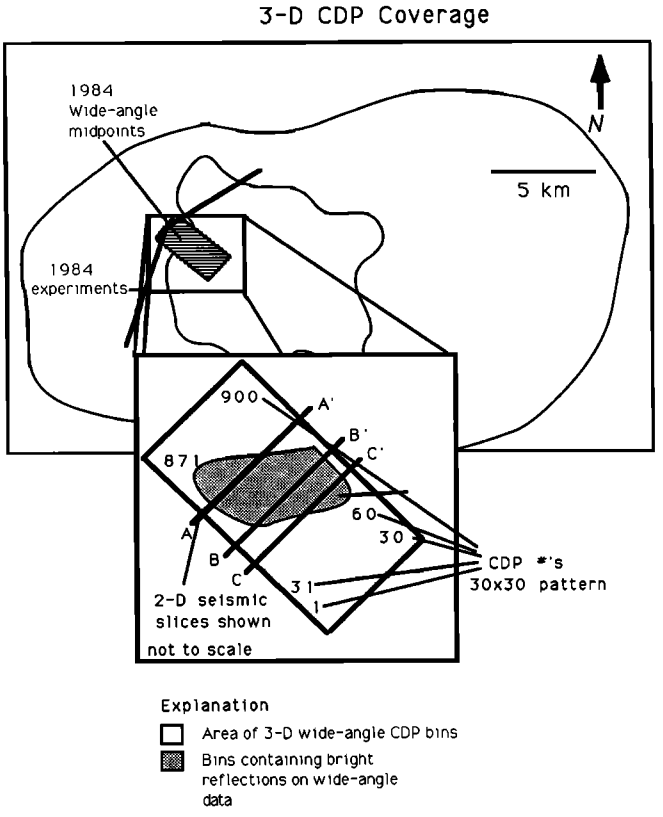

Fig. 10. Map view of three-dimensional (3-D) midpoint area showing distribution of CDP bins and areal extent of events in 3-D stacked section. Note the relatively small areas covered by the high-amplitude reflections. This area is less than the area of the first Fresnel zone for the travel times and frequencies of interest. The locations of the cross sections of Figure 11 are also shown.

GENERALIZED CELLULAR MIGRATION

In order to find the true spatial position of the bright events observed on the wide-angle records, a new migration scheme, generalized cellular migration (GCM), was developed. The theory of the GCM technique is outlined here, but a full discussion of the method is presented by *Black* [1990].

The GCM method is a prestack migration algorithm utilizing only event arrival times. The technique calculates the probability that any subsurface location is a reflecting location, given the set of observed arrival times and a subsurface velocity model. The subsurface is represented by a three-dimensional grid of cells with individual seismic velocities, similar to velocity models used in tomographic applications. Each cell center represents a possible reflector location. The observed travel time between a given shot and receiver, picked from the shot record, is compared to a calculated travel time for each cell center. The calculated travel time represents the theoretical travel time from the shot to the cell center and back to the receiver. This travel time may be calculated along a ray-traced path using an algorithm optimized for cellular regions, such as the algorithms of *Langan et al.* [1985], or simply by applying Snell's Law at each of the cell boundaries. If the difference between the observed and calculated times is less than some threshold value, the cell is flagged as a possible reflector location.

Since each cell is tested as a possible reflector location for each shot-receiver pair, some cells will clearly be flagged as possible reflector locations many times, while some will not be flagged at all. The cell locations that are flagged the most times are the cells which have the highest probability of being reflector locations [*Black*, 1990]. This can be stated as

$$P(c_j|E)=[P(E|c_j)P(c_j)]/\sum_{i=1}^{N}[P(E|c_i)P(c_i)] \quad (1)$$

where $P(c_j|E)$ is the probability that cell j is the reflector location given the vector E of travel times for all seismic traces. Again, this probability is highest for the cells which are flagged by the most seismic traces. Equation (1) is simply Bayes Theorem, a basic theorem in probability theory [*Helstrom*, 1984]. The term on the right-hand side of the equation is a function of a conditional probability and an a priori probability. In the simplest case, where no a priori information is available concerning the reflector location (the usual case), the a priori probability can be written as

$$P(c_j)=1/N \quad (2)$$

where N is the total number of cells in the subsurface velocity model. This is a constant for any given model and can be factored out of the denominator in equation (1). Since it occurs in both the numerator and denominator in that equation, it cancels out, and the final probability values are simply a function of the conditional probability. The conditional probability, in this case, is the joint probability of the conditional probabilities due to each of M seismic traces:

$$P(E|c_j)=P(E_0|c_j)P(E_1|c_j)\ldots P(E_M|c_j) \quad (3)$$

where:

$$P(E_K|c_j)=K(E_k|c_j)/\sum_{i=1}^{N}K(E_k|c_i) \quad (4)$$

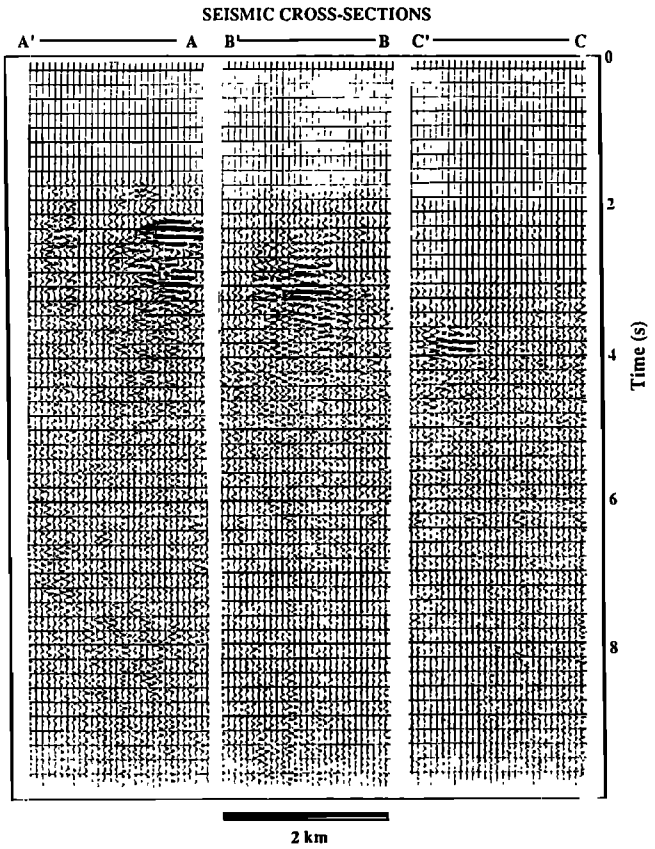

Fig. 11. Two-dimensional cross sections through three-dimensional (3-D) relative amplitude stack. The cross section locations are shown on Figure 10. These stacked sections show clearly that the bright events between about 2 and 4 s are much higher in amplitude than other energy in the section. However, the stacking velocity and 3-D event extent indicate that these events may actually be due to reflections from out of the midpoint region.

The K terms are constants defined by:

$$K(E|c_j)=1.0 \text{ if } c_j \text{ was flagged by trace } k$$
$$K(E|c_j)=0.1 \text{ if } c_j \text{ was not flagged by trace } k \quad (5)$$

These constants are somewhat arbitrary but reflect the fact that a cell center with a proper calculated travel time is much more likely to be the true reflector location than a cell center with a calculated travel time that differs greatly from the observed time on some seismic trace k. The constants shown (1.0 and 0.1) seismic trace k. The constants shown (1.0 and 0.1) have the nice property that the final probabilities found using equation (1) will be a simple exponential function of the number of traces which flagged the cell. This can be stated as

$$\log_r[P(c_j|E)]=aF_j \quad (6)$$

where the base r is the ratio of flagged over unflagged conditional probabilities, F_j is the number of times that cell j was flagged during the analysis and a is some constant of proportionality. Thus a plot of the number of times each cell was flagged during the analysis is also an image of the logarithm of the relative probability that each cell contains a reflector (scaled by some constant of proportionality). The convenience of manipulating base 10 logarithms is the main reason for preferring the use of a ratio of 10 in the assignment of constants in equation (5). The probability image generated by this type of analysis is equivalent to (and just as simple to interpret as) the reflectivity image generated by standard reflection analyses or the velocity image generated in tomographic applications.

APPLICATION OF THE GCM METHOD

In order to apply the GCM technique to the bright reflection events it was first necessary to develop a subsurface velocity model for the area near the seismic experiment. A layered one-dimensional (1-D) velocity model (Figure 12) was chosen based on a simplification of the refraction velocities of *Hill et al.* [1985*a*]. The simple 1-D structure of the model was chosen so that any lateral changes in reflector probability could be directly tied to the arrival time data and so that any areas of concentrated high probability could not be dismissed as artifacts of the lateral velocity variations in the model. In addition, the layered velocity structure allows a very large model to be analyzed efficiently since fast ray-tracing algorithms can be utilized.

Observed travel times for the bright events (i.e., Figure 13) were picked by digitizing amplitude peaks on every fifth shot record along the wide-angle line. Sampling in this manner

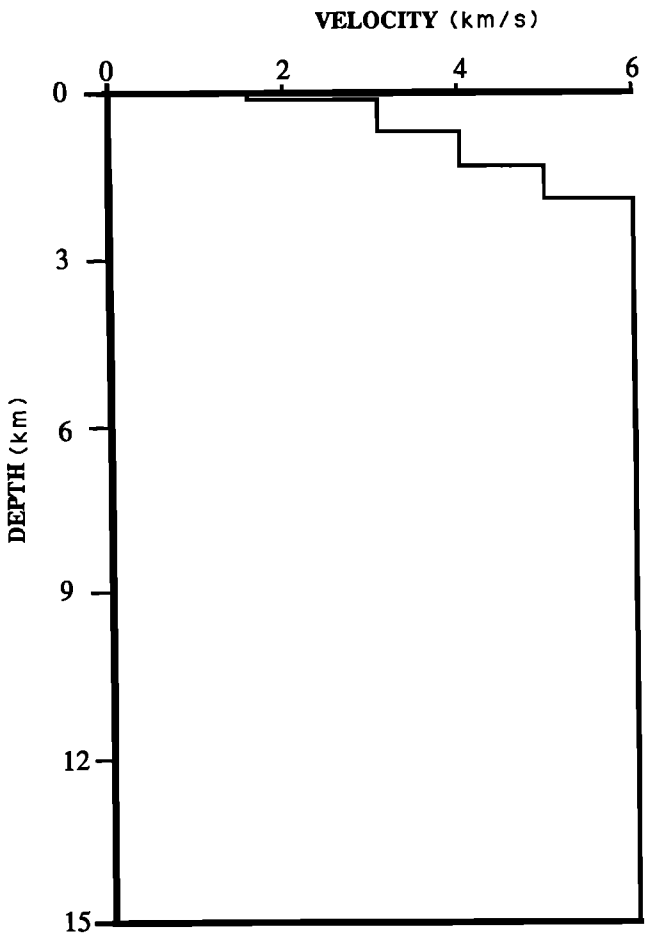

Fig. 12. Velocity model used in Long Valley GCM analysis. This model was adapted from refraction results of *Hill et al.* [1985*a*] and reflection results from the current study.

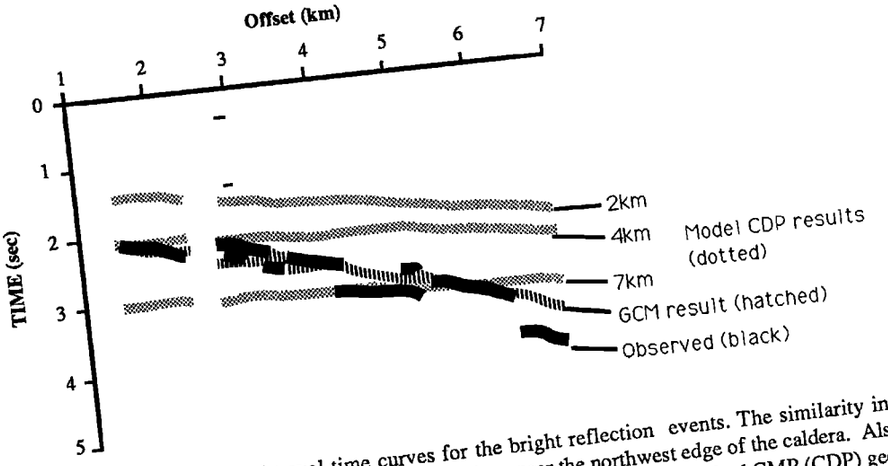

Fig. 13. Observed and GCM derived travel time curves for the bright reflection events. The similarity in the curves indicates that the reflection events probably arise from somewhere near the northwest edge of the caldera. Also shown are travel time curves for reflections from depths of 2, 4, and 7 km calculated assuming standard CMP (CDP) geometries are correct. The observed move-out curve is unlike any of the curves associated with reflections from within the midpoint rectangle, indicating that the reflections cannot be coming from the CMP area.

allowed redundant coverage over the full range of offsets while limiting the number of travel times to be analyzed to a few hundred. Such a limitation allowed the migration to be performed on a workstation-class computer. The digitized arrival times were compared to calculated arrival times for each cell in the subsurface model and probabilities calculated.

The output of the GCM algorithm indicated that an area along the northwestern portion of the caldera ring fracture system is the area with the highest probability of containing a reflector (Figure 14). The locations of highest probability were very shallow, ranging in depth from 0.3 to 1.0 km (Figure 15). The base-10 logarithm of the probability that the reflection events arise from this general location is approximately 60 times higher than the logarithm of the probability that they arise from the CDP locations used in the more standard 3-D CDP processing utilized in the previous sections of this paper.

This location indicates that the reflections are indeed coming from within the caldera, but at or near the structural edge of the feature. Since the ring fracture system was intentionally excluded from the velocity model, and since each cell had an equal a priori

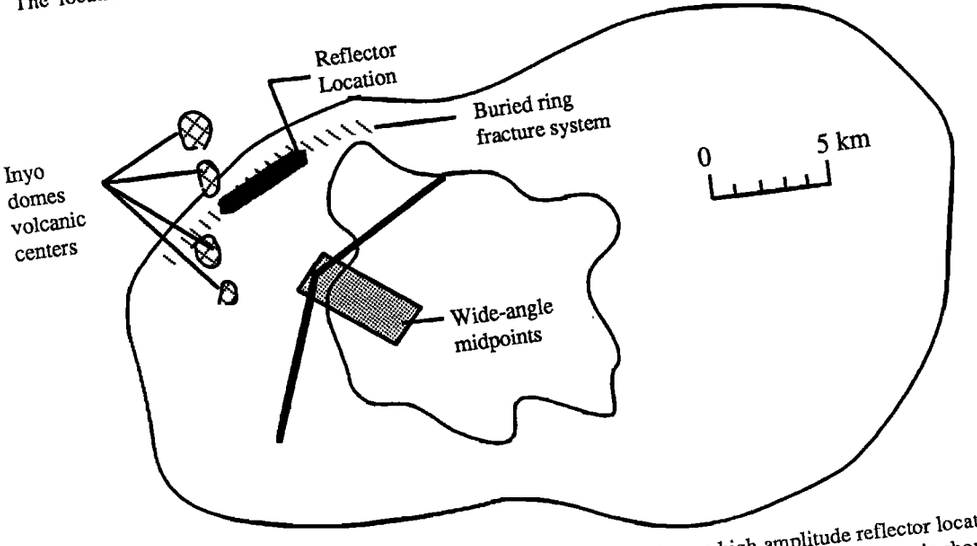

Fig. 14. Location of 1984 wide-angle midpoints (light stipple) and probable true high amplitude reflector location (dark stipple) determined from GCM analysis. Approximate subsurface location of the ring fracture system is shown by the diagonal patterned line. Geometric constraints indicate that the reflection is probably associated with the ring fracture system. However, the highly reflective area is very close to the most recently active eruptive centers within the caldera, the Inyo craters system.

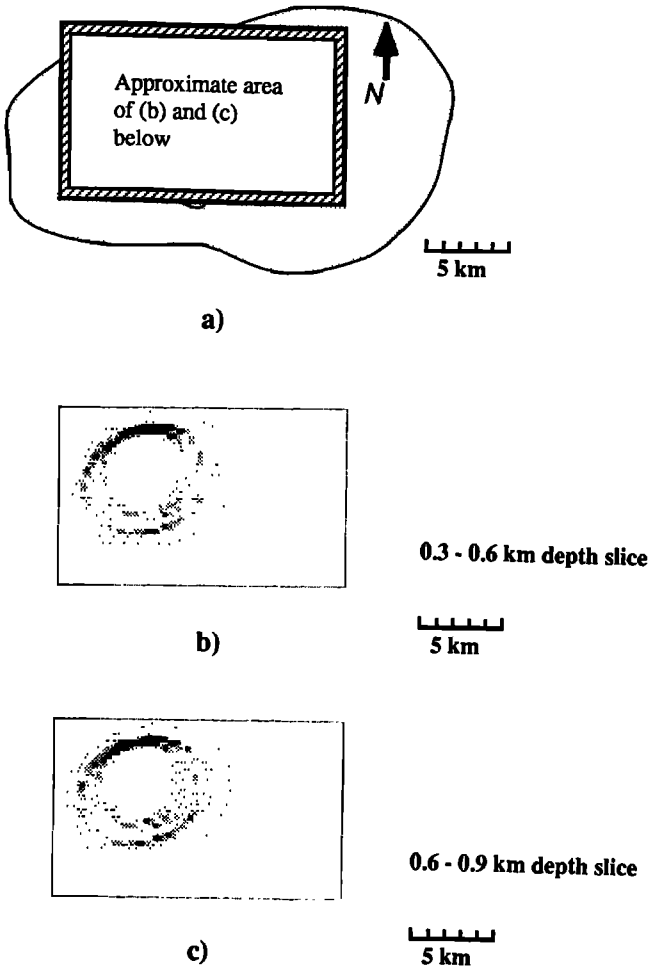

Fig. 15. (a) Location of the area utilized in the GCM analysis, and (b)-(c) depth slices of the log-probability image produced by the migration. Dark areas have the highest probability of containing the reflector. The migration delineated the northwestern portion of this area (Figure 14), at depths of less than 1 km, as the reflector location. Because of the pseudo-three-dimensional nature of the wide-angle survey geometry, the "mirror" image often produced by the three-dimensional migration of two-dimensional data was greatly attenuated.

probability of being a reflecting location, the concentration of high probabilities must be completely due to information contained in the arrival times of the bright reflectors. Subsets of the picks were isolated on the basis of their arrival time and each subgroup of time picks migrated to the same general area. Furthermore, the travel time curve calculated for the highest probability cells along the ring fracture system (Figure 13) have a move-out very similar to that of the observed travel time curve. Conversely, theoretical travel time curves for midpoint reflections at various depths (Figure 13) show little correspondence to the observed travel time curve.

In model studies using the GCM method, mirror image artifacts are often observed. Such artifacts are particularly strong when performing a three-dimensional migration of reflection times arising from out of the plane of a two-dimensional line with no lateral control [*Black*, 1990]. Mirror image artifacts were observed in the Long Valley migration (Figure 15) but were quite weak. The artifacts were attenuated due to the bend in the recording geometry (Figure 1) and the associated pseudo-three-dimensional spread of the raypaths (Figure 10).

The results of all of the migrations and ray tracing experiments performed for this study indicate that the high-amplitude events seen on the records are due to reflections from interfaces associated with the caldera ring fracture system at depths between 0.3 and 1.0 km. At these depths the faults associated with the ring fracture system may juxtapose relatively unconsolidated caldera fill (velocity less than 3.0 km/s) against crystalline Sierran basement (velocity around 4.5 to 5 km/s). A velocity contrast of this magnitude could easily explain the bright events without calling on magma bodies in the interpretation. The reflection coefficient associated with the ring fracture system, using velocities of 3.0 and 5.0 km/s and appropriate densities, would be approximately 0.3, similar to the apparent reflection coefficients calculated in previous studies of crustal "magma" reflectors [*Brocher*, 1981; *Serpa and deVoogd*, 1987]. It should be pointed out, however, that the results do not eliminate the possibility that the events are being caused by reflections from one or more melt-basement interfaces. In this unlikely scenario, however, the general location of the melt would be constrained to be within a dikelike body between 0.3 and 1.0 km in depth along the northwestern edge of the caldera.

DISCUSSION AND CONCLUSIONS

The Long Valley seismic reflection experiments have yielded several important results. The use of vibroseis data acquisition techniques within the geologically complex caldera moat yielded shallow crustal information in the western moat, where there is a strong acoustic impedence contrast associated with the caldera fill-basement interface. This interface shows up clearly as a continuous reflector on standard CDP data within the western moat (Figure 3). These positive results indicate that the CDP technique could be used for detailed mapping of the top of Sierran basement within most of the caldera, if such detailed information was deemed necessary for purposes of geothermal exploration or for seismic hazard accessment.

Recent work on the hydrothermal system [*Blackwell*, 1985; *Sorey*, 1985, 1987] indicates that the unit immediately above the basement, the welded Bishop Tuff, is the key hydrothermal aquifer in this portion of the caldera and that faults disrupting this unit are probably the main geothermal conduits between the deep aquifer and the near-surface aquifer system. Our work shows that the reflection technique can certainly be used to image the structural features of the deep aquifer system within the environment of Long Valley caldera. Because most silicic calderas seem to have generally similar geological histories, the CDP results indicate that the method should also work in other silicic caldera environments to provide information on caldera fill geometries, faulting, and intrusion history.

The refraction interpretation along the CDP line (Figure 8) clearly shows the presence of what can be interpreted as deeply incised paleochannels or a graben system. These interpreted features are at the same depth as the shallow hydrothermal aquifer [*Sorey*, 1985, 1987] from which an active geothermal power plant in the area produces its power. Although these features are farther west than known occurrences of the shallow hydrothermal aquifer, the results indicate that shallow refraction analyses associated with a CDP experiment could be used to investigate the subsurface geological controls on the distribution of the producible geothermal resources.

The major goal of the seismic experiments was to image the hypothesized magma body beneath the caldera. Although the signal from the vibrators was clearly detectable at offsets of 13 km, indicating that the source energy was adequate to reach midcrustal levels, at least three different investigators [*Deemer*, 1985; *Berg*, 1988; and this study] have sifted through the Long Valley caldera seismic reflection data discussed here, and found little or no evidence that strong magma reflectors exist in the areas expected from previous studies. Even though very bright events exist on the wide-angle data at travel times which, at first glance, seem to indicate that the events could be intrabasement "magmatic" reflections, migration of these events shows that they probably do not result from reflection from intrabasement interfaces at the shot-receiver midpoints but from very strong acoustic impedance contrasts associated with an area near the northwestern portion of the caldera wall (Figure 14). There are probably large buried fault scarps associated with the ring fracture system in the immediate area of the preferred reflector locations [*R.A. Bailey*, personal communication, 1987]. At depths less than 1 km these faults juxtapose relatively low-density, low-velocity caldera fill against unweathered crystalline rocks. Such a contact could easily have an associated reflection coefficient of 0.3 or greater. However, the large apparent reflectivity associated with the events could also be generated by juxtaposition of a melt against the crystalline country rock in the same location. Although the migrated reflector location is not directly along strike of the most recent chain of volcanic features, the Mono-Inyo crater system (Figure 14), it is quite close to the location where the buried ring fracture system probably intersects the dike which fed the Mono-Inyo system [*Fink*, 1985]. However, there is little chance that a small, shallow melt body associated with this dike system could now exist, since the main body of the larger dike has been shown to be completely crystallized [*Fink*, 1985].

In any continental, extensional area there are probably numerous range-bounding faults along which relatively unconsolidated sediments are juxtaposed against high-velocity materials. The results from Long Valley should raise a caution flag concerning interpretation of relatively deep "magma" reflectors from time ranges consistent with lateral travel times across extensional basins where 3-D control is unavailable.

Acknowledgments. We thank Richard Berg for his many contributions to the Long Valley project. We also wish to thank Dave Hill, Roy Bailey, Roy Johnson, Leon Borgman, and Walter Mooney for their advice and cooperation throughout the course of the project. We thank Dave Hill, Tom Brocher, Berndt Milkereit, and the editorial staff of the Journal of Geophysical Research for their patience and their detailed reviews. This work was supported by grants GS-14-08-0001-21956 and LBL-P.O.-4539310.

REFERENCES

Bailey, R. A., Relationship between basement geology, faults, and volcanic vents, Long Valley caldera, eastern California (extended abstract) in *Proceedings of the Symposium on the Long Valley Caldera: A Pre-Drilling Data Review*, pp. 1-7, Lawrence Berkeley Laboratory, Berkeley, Calif., 1987.

Bailey, R. A., G. B. Dalrymple, and M. A. Lanphere, Volcanism, structure, and geochronology of Long Valley caldera, Mono County, California, *J. Geophys. Res.*, *81*, 725-744, 1976.

Berg, R. S., Analysis of Seismic Reflection Data in Long Valley Caldera, California, M.S. thesis, 120 pp., Univ. of Wyo., Laramie, 1988.

Black, R. A., Seismic Imaging in Long Valley Caldera with Generalized Cellular Migration, Ph.D. dissertation, 104 pp., Univ. of Wyo., Laramie, 1990.

Blackwell, D. D., A transient model of the geothermal system of Long Valley caldera, California, *J. Geophys. Res.*, *90*, 11229-11242, 1985.

Brocher, T. M., Geometry and physical properties of the Soccoro, New Mexico, magma bodies, *J. Geophys. Res.*, *86*, 9420-9432, 1981.

Brocher, T. M., and R. A. Phinney, A ray parameter- intercept time spectral ratio method for seismic reflectivity analysis, *J. Geophys. Res.*, *86*, 7845-7873, 1981.

Carle, S. F., and N. E. Goldstein, A three-dimensional gravity model of the geologic structure of Long Valley caldera (extended abstract), in *Proceedings of the Symposium on the Long Valley Caldera: A Pre-Drilling Data Review*, pp. 122-135, Lawrence Berkeley Laboratory, Berkeley, Calif., 1987.

Deemer, S. J., Seismic Reflection Profiling in the Long Valley Caldera, California: Data Acquisition, Processing and Interpretation, M.S. thesis, 195 pp., Univ. of Wyo., 1985.

Detrick, R. S., P. Buhl, E. Vera, J. Mutter, J. Orcutt, J. Madsen, and T. Brocher, Multi-channel seismic imaging of a crustal magma chamber along the East Pacific Rise, *Nature*, *326*, 35-41, 1987.

Fink, J. H., Geometry of silicic dikes beneath the Inyo Domes, California, *J. Geophys. Res.*, *90*, 11127-11133, 1985.

Hale, L. D., C. J. Morton, and N. H. Sleep, Reinterpretation of seismic reflection data over the East Pacific Rise, *J. Geophys. Res.*, *87*, 7707-7717, 1982.

Helstrom, C. W., *Probability and Stochastic Processes for Engineers*, 328 pp., Macmillan, New York, 1984.

Hermance, J. F., Characterizing thermal energy and mass transport in volcanic caldera complexes; the role of scientific drilling, in *Observation of the Continental Crust through Drilling I*, edited by C. B. Raleigh, Springer-Verlag, New York, 1985.

Herron, T. J., W. J. Ludwig, P. L. Stoffa, T. K. Kan, and P. Buhl, Structure of the East Pacific Rise from multichannel seismic reflection data, *J. Geophys. Res.*, *83*, 798-804, 1978.

Hill, D. P., Structure of Long Valley, caldera, California, from a seismic refraction experiment, *J. Geophys. Res.*, *81*, 745-753, 1976.

Hill, D. P., E. Kissling, J. H. Luetgert, and U. Kradolfer, Constraints on the upper crustal structure of the Long Valley-Mono Craters volcanic complex, eastern California, from seismic refraction measurements, *J. Geophys. Res.*, *90*, 11135-11150, 1985a.

Hill, D. P., R. A. Bailey, and A. S. Ryall, Active tectonic and magmatic processes beneath Long Valley caldera, eastern California: An overview, *J. Geophys. Res.*, *90*, 11111-11120, 1985b.

Lachenbruch, A. H., J. H. Sass, R. J. Munroe, and T. H. Moses, Jr., Geothermal setting and simple heat conduction models for the Long Valley cladera, *J. Geophys. Res.*, *81*, 769-784, 1976.

Langan, R. T., I. Lerche, and R. T. Cutler, Tracing of rays through heterogeneous media: An accurate and efficient procedure, *Geophysics*, *50*, 1456-1466, 1985.

Morton, J. L., and N. H. Sleep, Seismic reflections from a Lau Basin magma chamber, in *Geology and Offshore Resources of Pacific Island Arcs-Tonga Region, Earth Science Ser.*, vol. 2, edited by D. W. Scholl and T. L. Vallier, Circum-Pacific Council for Energy and Mineral Resources, pp. 441-453, Houston, Tex., 1985.

Morton, J. L., N. H. Sleep, W. R. Normark, and D. H. Tompkins, Structure of the Southern Juan de Fuca Ridge from seismic reflection records, *J. Geophys. Res.*, *92*, 11315-11326, 1987.

Muffler, L. J. P., and D. L. Williams, Geothermal investigations of the U.S. Geological Survey in Long Valley, California, 1972-1973, *J. Geophys. Res.*, *81*, 721-724, 1976.

Palmer, D., The generalized reciprocal method of refraction seismic interpretation, *Geophysics*, *46*, 1508-1518, 1981.

Sanders, C. O., Location and configuration of magma bodies beneath Long Valley, California, determined from anomalous earthquake signals, *J. Geophys. Res.*, *89*, 8287-8302, 1984.

Savage, J. C., and R. S. Cockerham, Earthquake swarm in Long Valley caldera, California, January 1983, evidence for dike intrusion, *J. Geophys. Res.*, *89*, 8315-8324, 1984.

Savage, J. C., R. S. Cockerham, J. E. Estrem, and L. R. Moore, Deformation near Long Valley caldera, Eastern California, 1982-1986, *J. Geophys. Res.*, *92*, 2721-2746, 1987.

Serpa, L., and B. deVoogd, Deep seismic reflection evidence for the role of extension in the evolution of the continental crust, *Geophys. J.R. Astron. Soc.*, *89*, 55-60, 1987.

Sorey, M.L., Evolution and present state of the hydrothermal system in Long Valley caldera, *J. Geophys. Res.*, *90*, 11219-11228, 1985.

Sorey, M. L., Overview of the Long Valley hydrothermal system (extended abstract), in *Proceedings of the Symposium on the Long Valley Caldera: A Pre-Drilling Data Review*, pp. 8-11, Lawrence Berkeley Laboratory, Berkeley, Calif., 1987.

Sorey, M. L., R. E. Lewis, and F. H. Olmsted, The hydrothermal system of Long Valley, California, *U.S. Geol. Surv. Prof. Pap.*, *1044-a*, 60pp., 1978.

Steeples, D. W., and H. M. Iyer, Low-velocity zone under Long Valley as determined from teleseismic events, *J. Geophys. Res.*, *81*, 849-860, 1976.

Sumnicht, G. A., and R. J. Varga, Constraints on models of structure and hydrothermal circulation in Long Valley caldera, California (extended abstract), in *Proceedings of the Symposium on the Long Valley Caldera: A Pre-Drilling Data Review*, pp. 32-38, Lawrence Berkeley Laboratory, Berkeley, Calif., 1987.

deVoogd, B., L. Serpa, L. Brown, E. Hauser, S. Kaufman, J. Oliver, B. W. Troxel, J. Willemin, and L. A. Wright, Death Valley bright spot: A midcrustal magma body in the southern Great Basin, California?, *Geology*, *14*, 64-67, 1986.

R. A. Black, Department of Geology, 120 Lindley Hall, University of Kansas, Lawrence, KS 66045.

S. J. Deemer, Earthquake Station, University of Bergen, Bergen, Norway.

S. B. Smithson, Program for Crustal Studies, University of Wyoming, Laramie, WY 82071.

(Received December 11, 1989;
revised July 3, 1990;
accepted September 14, 1990.)